Supporting Information for

PCN-224-Pt Nanozyme for Dual-Mode Detection of Acetylcholinesterase via LMB-PEG

Weiyi Bai,‡[a] Ling Teng,‡[a] Xingzhi Yu,[a] Qing Li,[a] Huiling Tan,[a] Yongchao Yao,[a] Shufen Li,[b] Limei Zhang,[a] Hao Bai,[a] Imran Shakir,[c] Weihua Zhuang,[a]* Yuan Yang,[d]* Xuping Sun[e,f]* and Walter (Wenchuang) Hu[a]*

[a] Department of Laboratory Medicine, Precision Medicine Translational Research Center, Frontiers Science Center for Disease-related Molecular Network, West China Hospital, Sichuan University, Chengdu 610041, Sichuan, China.

[b] Laboratory of Cardiac Structure and Function, Institute of Cardiovascular Diseases, West China Hospital, Sichuan University, Chengdu 610041, Sichuan, China.

[c] Department of Physics, Faculty of Science, Islamic University of Madinah, Madinah 42351, Saudi Arabia.

[d] Department of Pathogen Biology, West China School of Basic Medical Sciences & Forensic Medicine, Sichuan University, Chengdu 610041, Sichuan, China.

[e] Center for High Altitude Medicine, West China Hospital, Sichuan University, Chengdu 610041, Sichuan, China.

[f] College of Chemistry, Chemical Engineering and Materials Science, Shandong Normal University, Jinan 250014, Shandong, China.

‡ Weiyi Bai and Ling Teng contributed equally to this work.

* Corresponding authors. E-mail addresses: weihuaz@scu.edu.cn (Weihua Zhuang), yang_yuan@scu.edu.cn (Yuan Yang), xpsun@uestc.edu.cn (Xuping Sun) and huwenchuang@wchscu.cn (Walter Hu).

Contents

References

Experimental Section

Materials: Zirconyl chloride octahydrate ($ZrOCl_2 \cdot 8H_2O$), benzoic acid, H_2TCPP, potassium chloroplatinate (K_2PtCl_6), Sodium carbonate (Na_2CO_3) and citric acid were purchased from Shanghai Bidepharm Pharmaceutical Technology Co., Ltd. (Shanghai, China). thiamine pyrophosphate (TPP), acetylthiocholine (ATCh), sodium acetate (NaAc) and 3,3′,5,5′-Tetramethylbenzidine (TMB) were purchased from Shanghai Aladdin Biochemical Technology Co. Ltd. (Shanghai, China). Disodium hydrogen phosphate (Na_2HPO_4), Acetylcholinesterase (AChE), acetic acid (HAc) and Methoxy polyethylene glycol amine **(**mPEG–NH_2) were purchased from Shanghai Macklin Biochemical Technology Co., Ltd. (Shanghai, China). All other chemicals were of analytical grade and were used as received. The solutions used in this work were prepared with ultrapure water (resistivity = 18.25 MΩ·cm).

Instruments: The structure and morphology of the prepared materials were characterized via transmission electron microscopy (TEM) (JEOL JEM-F200, 200 kV), energy-dispersive X-ray spectroscopy (EDS) (JEOL JEM-F200, 200 kV) and high-resolution transmission electron microscopy (HRTEM) (JEOL JEM-F200, 200 kV). Scanning electron microscopy (SEM) images were obtained via a Thermo Fisher Scientific Apreo 2S field emission scanning electron microscope. The average size of the nanoparticles (NPs) in the fluid state was estimated by measuring the particles in the SEM images via ImageJ software. X-ray diffraction (XRD) analysis was performed using a LabX XRD-6100 powder diffractometer (SHIMADZU, Japan) equipped with a Cu Kα radiation source. X-ray photoelectron spectroscopy (XPS) was performed on a Thermo Scientific Nicolet iD50 instrument. Fourier transform infrared (FTIR) spectroscopy was performed on a Thermo Fisher Scientific Vector 22. Ultraviolet–visible (UV–vis) testing was performed with a UV–visible instrument (Perkin Elmer LAMBDA 1050+) and fluorescence spectra were recorded using a fluorescence spectrophotometer (F-4700, Hitachi, Japan). Dynamic light scattering (DLS) and zeta potential (ZP) measurements were performed via Malvern Zetasizer Pro. Electron spin resonance (ESR) assay was performed with an ESR spectrometer (Bruker A300).

Synthesis of PCN-224-Pt: PCN-224 NPs were synthesized as previously reported.[1] Typically, 100 mg of H_2TCPP, 200 mg of $ZrOCl_2 \cdot 8H_2O$, and 2.8 g of benzoic acid were first dissolved in 100 mL of N, N-dimethylformamide (DMF). The mixture was subsequently heated at 90 ℃ with continuous stirring (300 rpm) for 5 h. The product was collected via centrifugation and washed with DMF three times, ethanol twice and dried for use. 6 mg of PCN-224 NPs were dissolved in 3 mL of water, and K_2PtCl_6 (10 mM, 240 μL) was added and stirred for 1 h. After that, 90 μL of $NaBH_4$ (4 mg mL^{-1}) was added rapidly and stirred vigorously for 3 h. Finally, the mixture was centrifuged, washed with water three times and resuspended in 2.5 mL of water to obtain platinum modified PCN-224-Pt.

Synthesis of LMB-PEG: LMB-Cl was synthesized according to previous work.[24] Under N_2 atmosphere, $mPEG_4–NH_2$ (0.30 g, 1.44 mmol) and trimethylamine (401 μL, 2.87 mmol) were dissolved in dichloromethane. The mixed solution was immersed in an ice bath, LMB-Cl (0.50 g, 1.44 mmol) dissolved in dichloromethane was added dropwise. The resulting solution was stirred at room temperature for 24 h. After reaction, the solvent was concentrated under vacuum. White LMB-PEG was obtained via flash column chromatography with dichloromethane/methanol as the eluent (1:20, V:V) (yield: 85%).^{1}H NMR (400 MHz, DMSO-d6): 7.25-7.28 (d, 2H), 6.70-6.71 (d, 2H), 6.64-6.67 (m, 4H), 5.90-5.93 (t, 1H), 3.48-3.50 (m, 10H), 3.39-3.42 (m, 4H), 3.22 (s, 3H), 3.16-3.20 (m, 2H), 2.89 (s, 12H) ppm. ^{13}C NMR (100 MHz, DMSO-d6): 155.59, 149.00, 133.57, 128.76, 127.75, 111.60, 110.77, 71.74, 70.28, 70.25, 70.06, 70.00, 69.63, 58.52, 40.71 ppm.

Zeta potential measurement procedure: PCN-224-Pt was dispersed in deionized water and sonicated for 5 min. Zeta potential was measured at 25°C using a Malvern Zetasizer Pro with a disposable folded capillary cell. Each sample was measured in triplicate. The same procedure was applied to the other samples.

The POD-Like Activity and Kinetic Assay of PCN-224-Pt: PCN-224-Pt-catalyzed oxidation reactions were performed in CBS buffer (0.1 M citric acid, 0.2 M Na_2HPO_4,

pH 4.0). 10 μL of 20 mM TMB and 20 μL of 2 M H_2O_2 were mixed with 160 μL of buffer, followed by the addition of 10 μL PCN-224-Pt (8 μg·mL^{-1}), and the absorbance at 652 nm was recorded. For kinetic studies, PCN-224-Pt (1.83 μg·mL^{-1}) and 10 μL of 5 M H_2O_2 were added to a 96-well plate, followed by varying concentrations of TMB (0–1500 μM) or LMB-PEG (0–1000 μM), and the absorbance changes at 652 nm or 665 nm were monitored. H_2O_2 kinetics were measured by varying its concentration (0–2500 mM) under fixed TMB (20 mM) and PCN-224-Pt (8 μg·mL^{-1}) conditions. The initial reaction velocity (v) was calculated from the absorbance change over time, using the molar absorption coefficient of the substrate (39,000 M^{-1}·cm^{-1} for ox-TMB and 84,000 M^{-1}·cm^{-1} for MB) and a path length of 0.6 cm. Michaelis-Menten parameters (V_{max} and K_m) were determined by plotting the initial reaction velocities against substrate concentrations and fitting the data using nonlinear regression.

ESR assay: The presence of hydroxyl radical (·OH) was determined by employing the signal capture agent 5,5-dimethyl-1-pyrroline-oxide (DMPO). A 30 μL aliquot of DMPO (100 mM) was introduced into a solution consisting of 1 mL HAc-NaAc buffer (0.2 M, pH 4.0), containing PCN-224-Pt at a concentration of 50 μg mL^{-1} and H_2O_2 at a concentration of 2 mM. Following a reaction period of 5 min, an ESR spectrometer was utilized to evaluate the generation of ·OH. All experimental procedures were carried out under ambient conditions.

Colorimetric and fluorescence detection of AChE activity: In the colorimetric mode, different AChE activity (25 μL, 0–100 mU mL^{-1}) were mixed wth ATCh (25 μL, 20 mM). To completely suppress its activity, PCN-224-Pt (10 μL, 9.15 μg mL^{-1}) was added after 30 min of incubation at 37 °C. Subsequently, 140 μL of CBS buffer (0.1 M citric acid, 0.2 M Na_2HPO_4, pH 4.0), 20 μL of H_2O_2 (20 mM), and 20 μL of LMB-PEG (1 mg mL^{-1}) were sequentially added. The absorbance (A) was recorded after 15 min, while A_0 was obtained from a parallel setup without ATCh. The experiment was replicated 3 times. Similarly, the TMB of the same concentration was also used for AChE activity detection, and the absorbance value at 652 nm was measured after 8 min. The fluorescence mode follows the same procedure as the colorimetric mode.

Colorimetric and fluorescence detection of TPP: In the colorimetric mode, TPP solutions of different concentrations (25 μL, 0–1000 μM) were combined with AChE (25 μL, 50 mU mL^{-1}) and incubated for 1 h. Subsequently, ATCh (25 μL, 20 mM) was added, the mixture was further incubated for 4 h. PCN-224-Pt (10 μL, 9.15 μg mL^{-1}) was added and incubated for 10 min to fully inhibit its activity. Then, CBS buffer (75 μL, 0.1 M citric acid, 0.2 M Na_2HPO_4, pH 4.0), H_2O_2 (20 μL, 20 mM), and LMB-PEG (20 μL, 1 mg mL^{-1}) were added sequentially. UV–vis was then used to measure absorption. The experiment was replicated 3 times. The fluorescence mode follows the same procedure as the colorimetric mode.

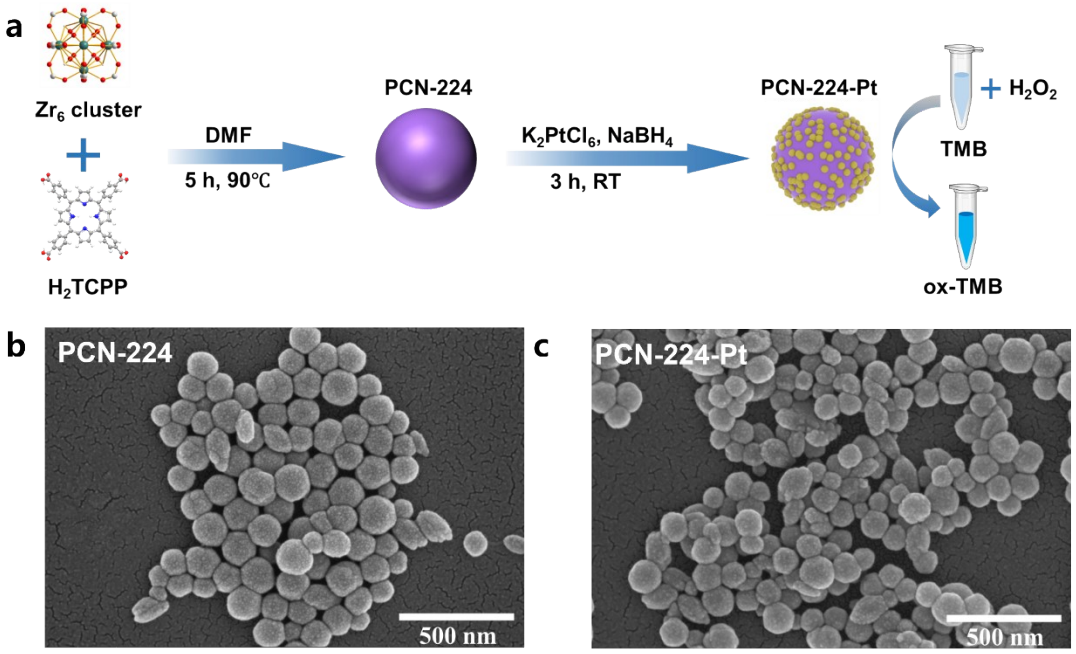

Figure S1. (a) Schematic of the synthesis of PCN-224-Pt. (b) SEM image of PCN-224 and (c) PCN-224-Pt. Scale bar: 500 nm.

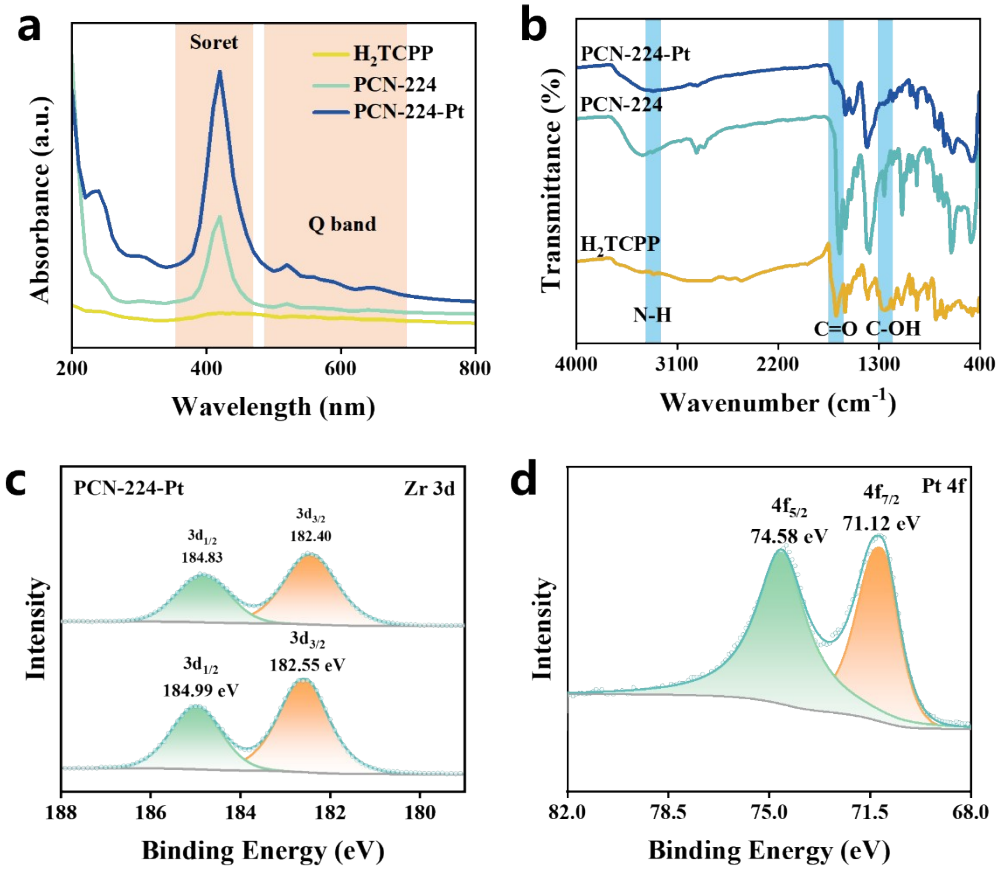

Figure S2. (a) UV–vis and (b) FTIR spectra of H_2TCPP, PCN-224, and PCN-224-Pt. (c) High-resolution XPS spectra of Zr in PCN-224 and PCN-224-Pt. (d) High-resolution XPS spectrum of Pt 4f in PCN-224-Pt.

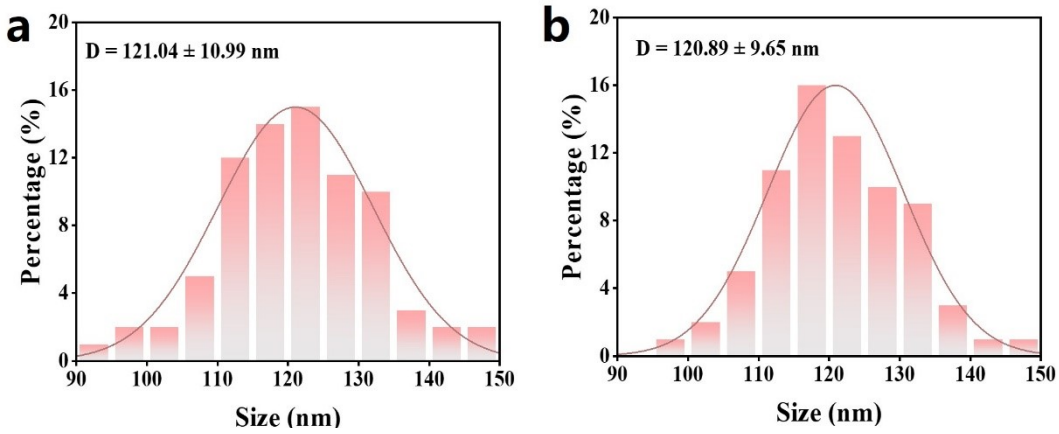

Figure S3. (a) Particle size statistics of PCN-224 and (b) PCN-224-Pt calculated from SEM image analysis.

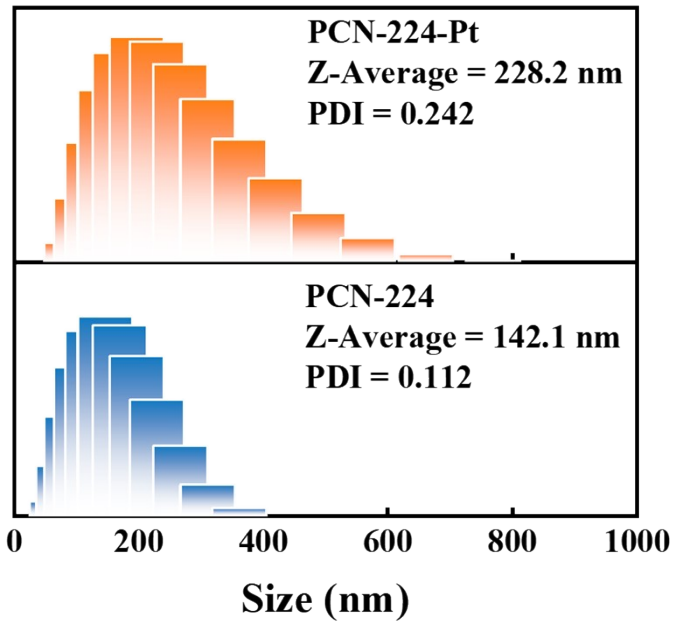

Figure S4. Comparison of hydrated particle size and PDI of PCN-224 and PCN-224-Pt.

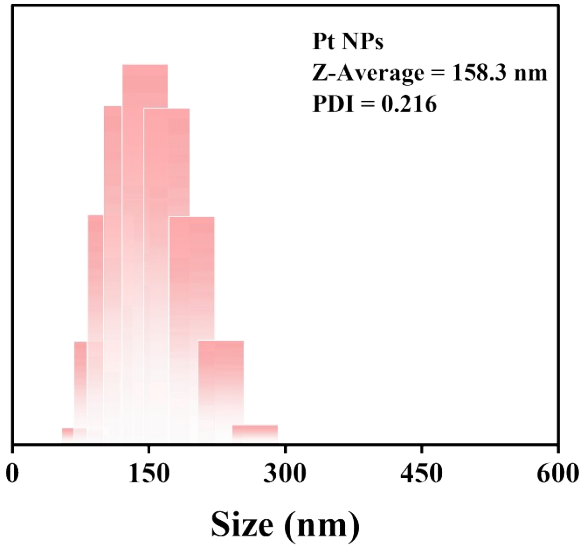

Figure S5. Hydrated particle size and PDI of Pt NPs.

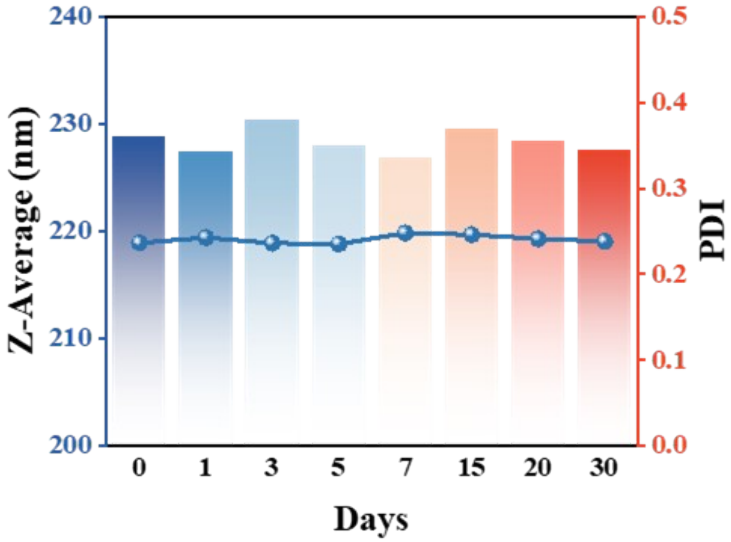

Figure S6. Hydrated particle size and PDI of PCN-224-Pt in 30 days.

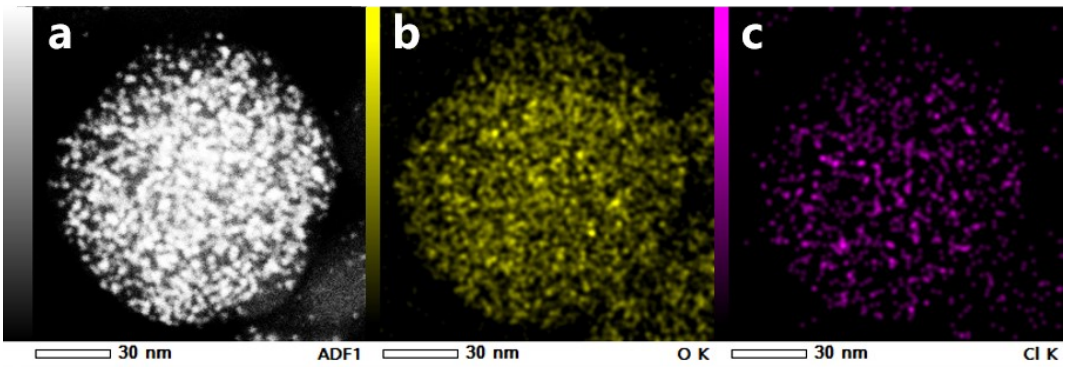

Figure S7. (a) HAADF image, (b) element O and (c) element Cl mapping images of PCN-224-Pt.

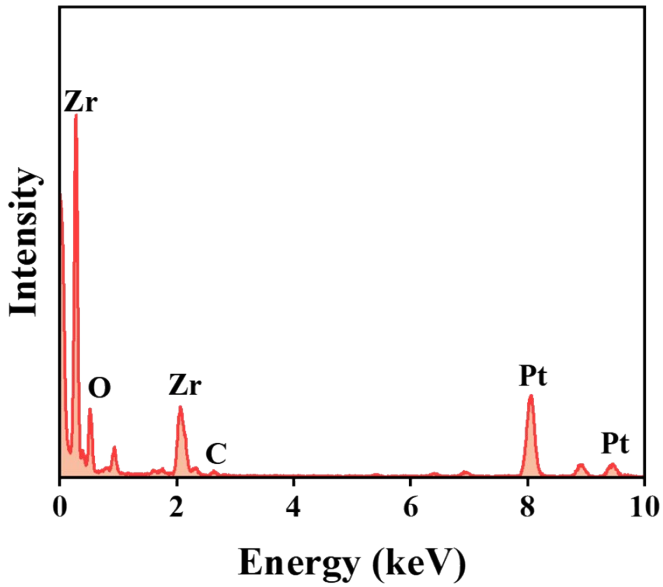

Figure S8. EDS spectrum of PCN-224-Pt.

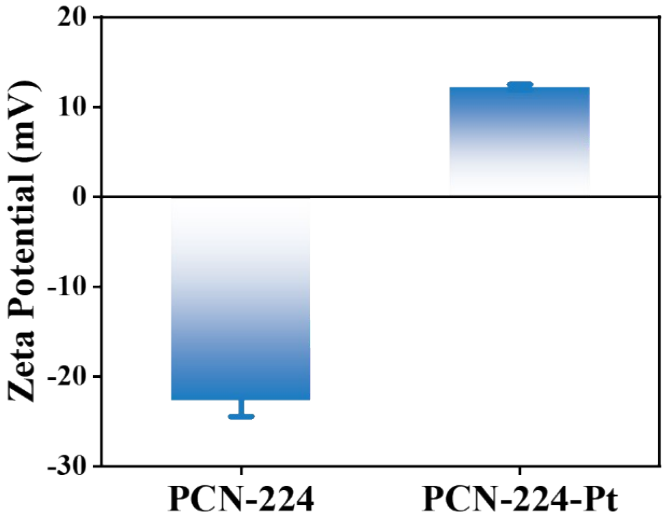

Figure S9. Comparison of zeta potentials of PCN-224 and PCN-224-Pt.

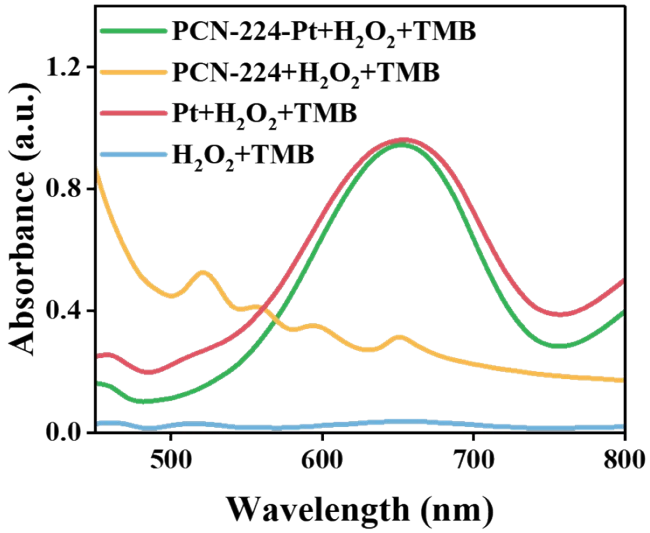

Figure S10. UV–vis spectra of TMB catalysis under four conditions: PCN-224-Pt, PCN-224, Pt NPs and without nanozyme.

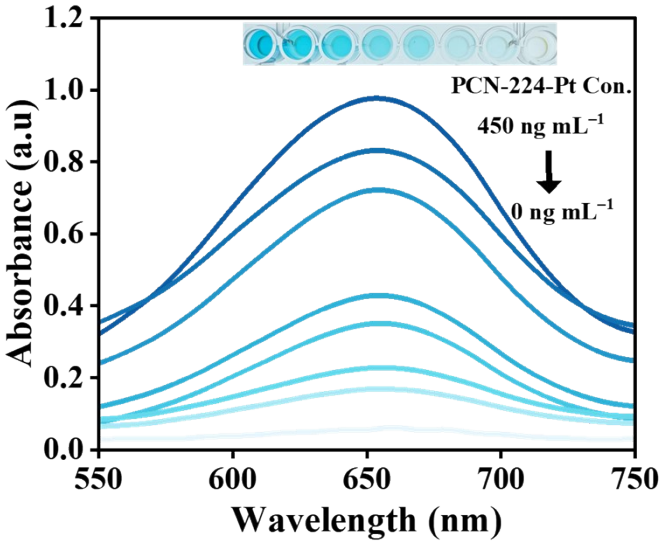

Figure S11. UV–vis spectra of TMB color development catalyzed by varying concentrations of PCN-224-Pt.

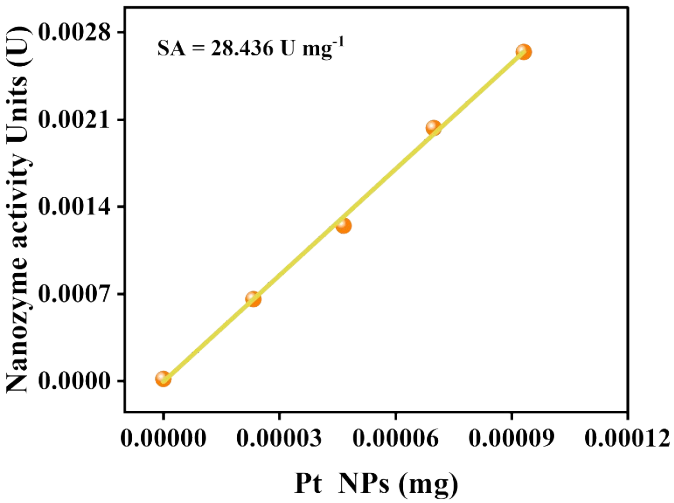

Figure S12. The specific activity of Pt NPs.

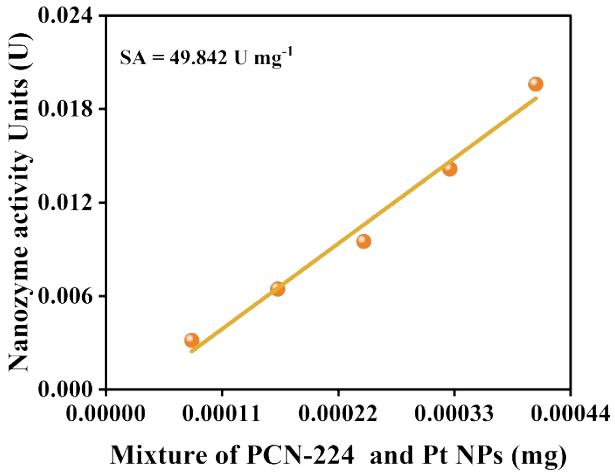

Figure S13. The specific activity of mixture of PCN-224 and Pt NPs.

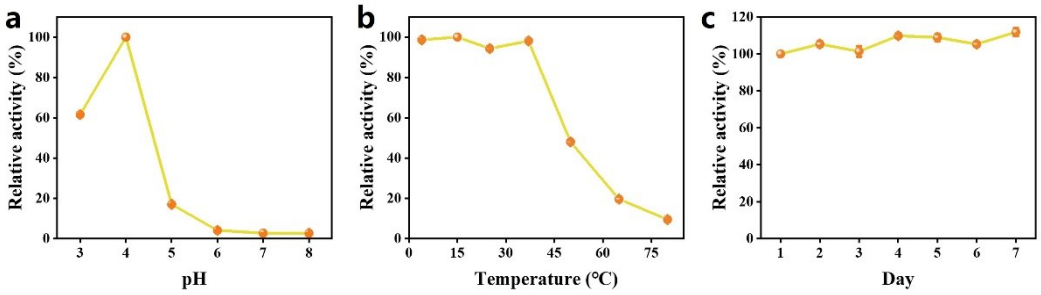

Figure S14. (a) pH stability and (b) temperature stability of the POD-like activity of PCN-224-Pt, with the highest activity under optimal conditions set as 100%. (c) The relative catalytic activity of PCN-224-Pt over 7 days at room temperature.

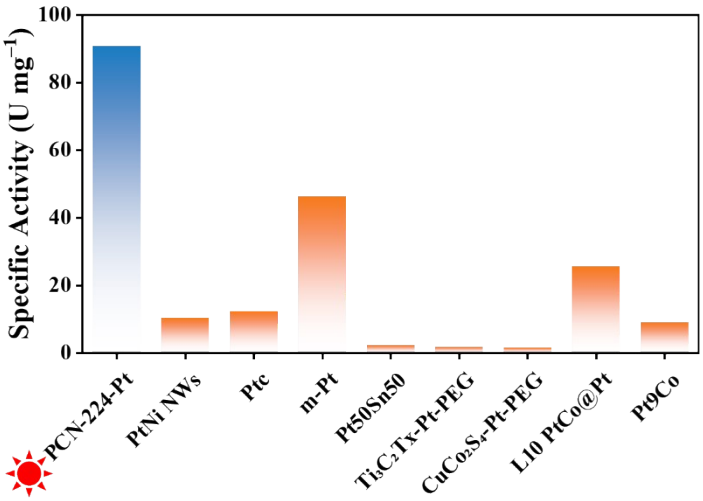

Figure S15. Comparative analysis of enzymatic activities between PCN-224-Pt and Pt nanozymes.

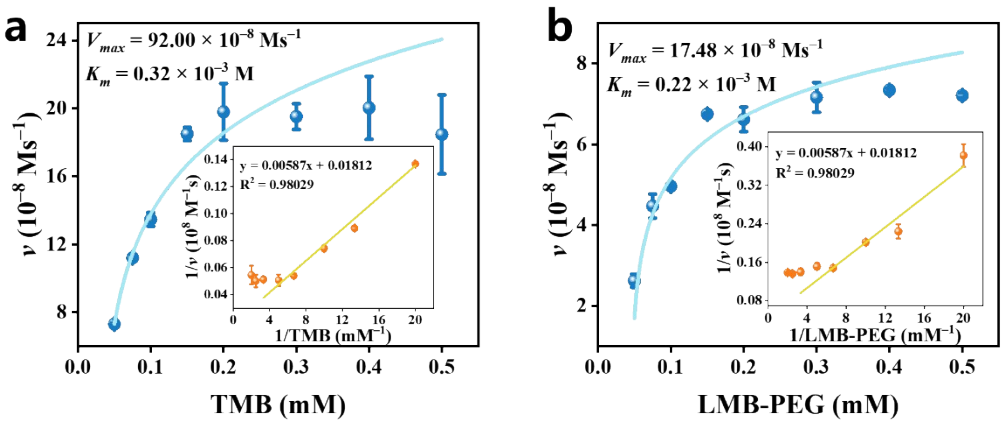

Figure S16. (a) Michaelis-Menten kinetics of Pt NPs fitted with TMB and (b) LMB-PEG as substrates (inset shows Lineweaver-Burk plots of the double reciprocal of the Michaelis-Menten equation).

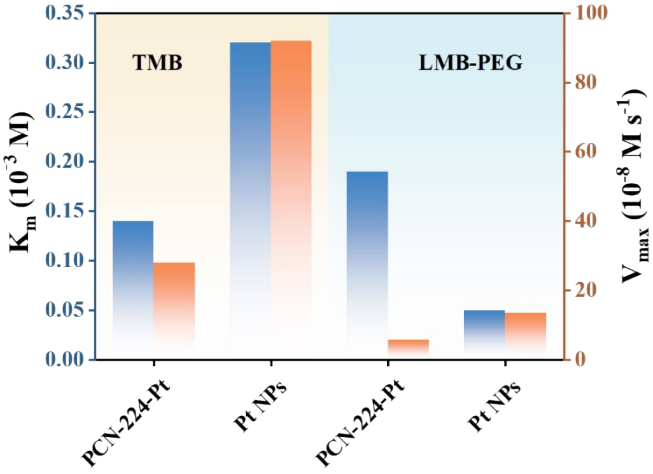

Figure S17. Comparison of K_m and V_{max} of PCN-224-Pt and Pt nanoparticles using LMB-PEG and TMB as substrates.

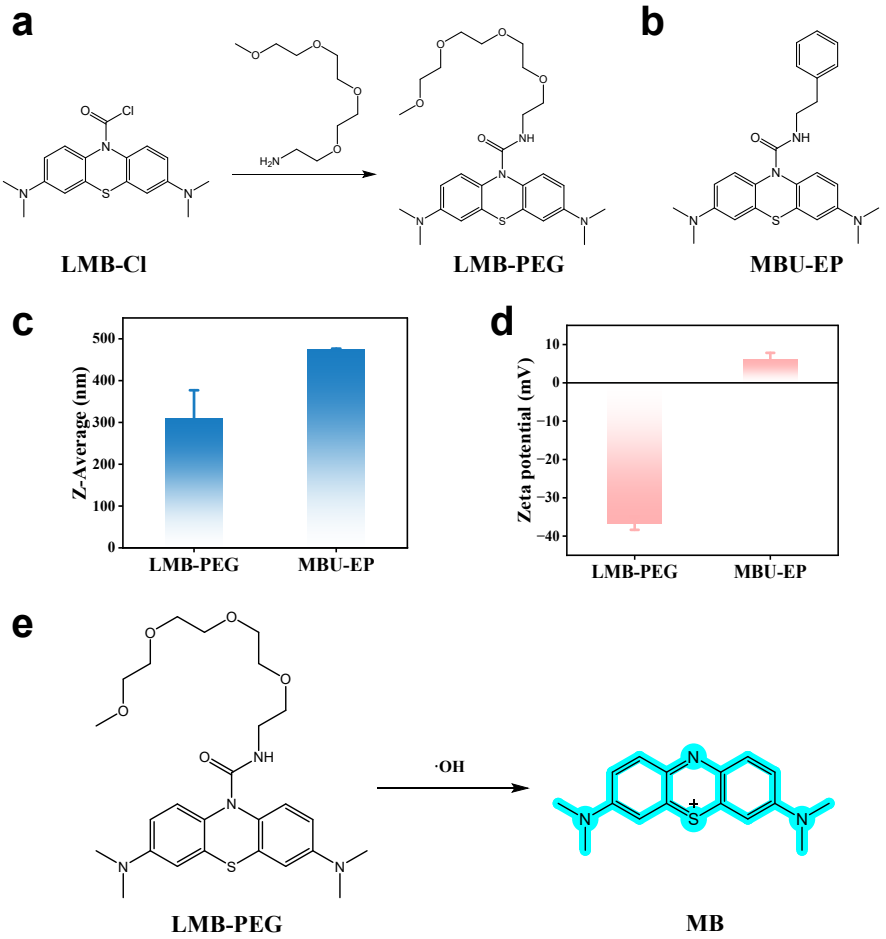

Figure S18. (a) Synthetic route of LMB-PEG. (b) Molecular structure of MBU-EP. (c) Comparison of the hydrated particle sizes and (d) the ζ-potential of LMB-PEG and MBU-EP. (e) Schematic diagram of LMB-PEG decomposition under the action of ·OH.

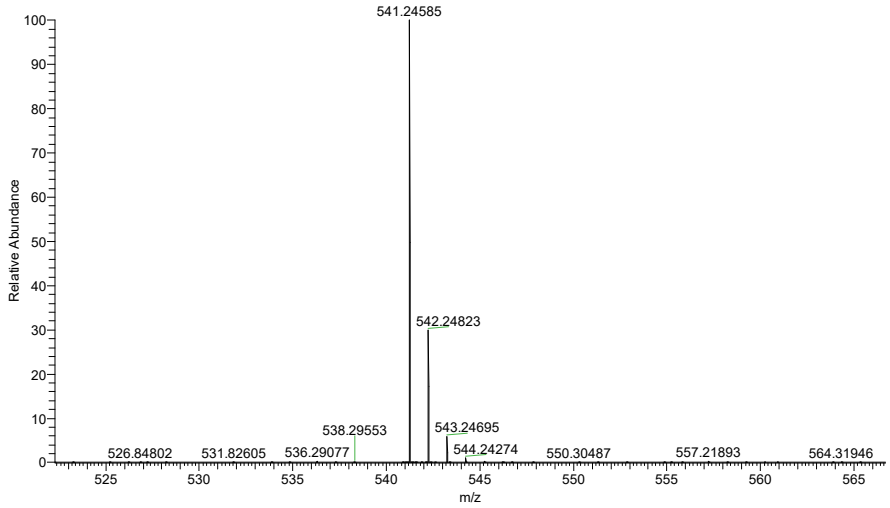

Figure S19. HRMS spectrum of LMB-PEG.

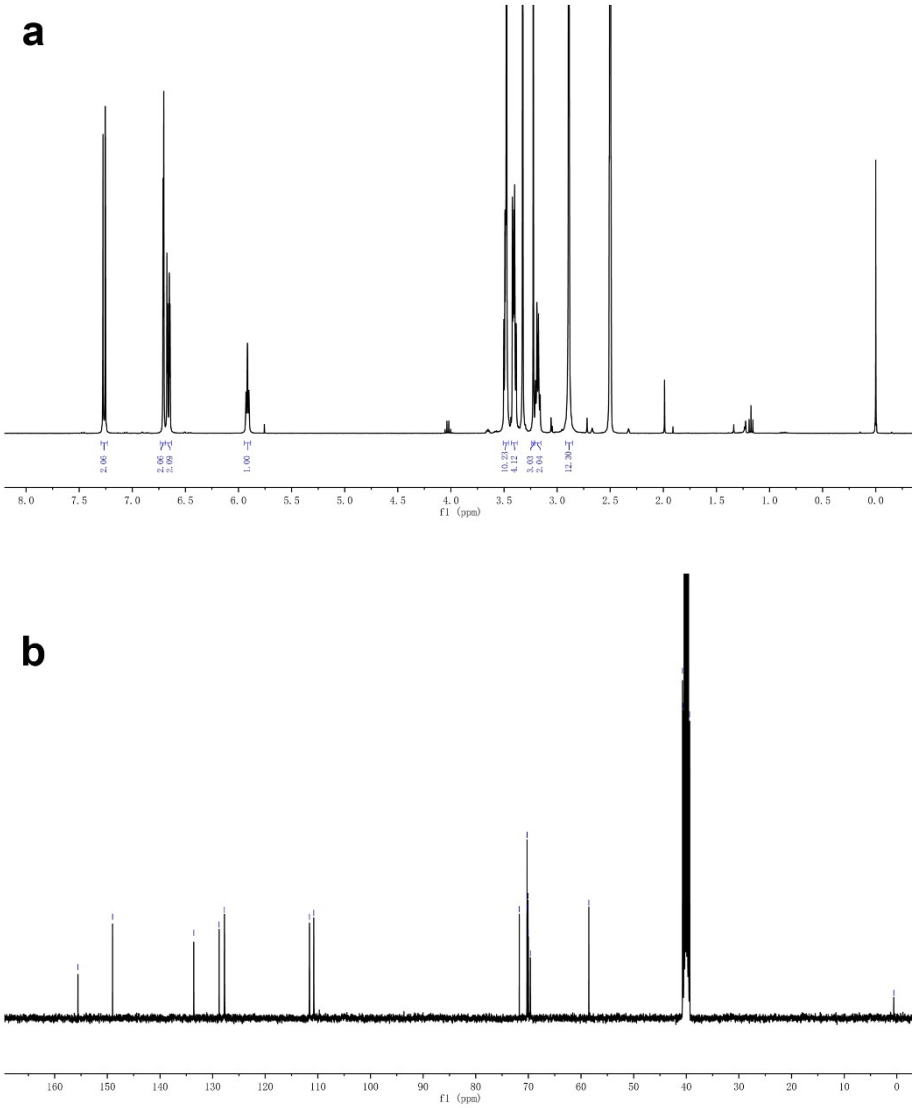

Figure S20. (a) ^{1}H NMR and (b) ^{13}C NMR spectrum of LMB-PEG in DMSO-d_6.

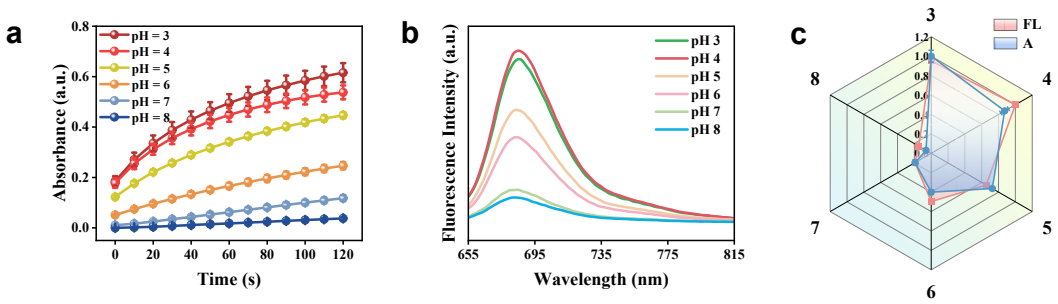

Figure S21. (a) pH-dependent absorbance kinetics of catalytic LMB-PEG oxidation. (b) pH-modulated fluorescence response of catalytic LMB-PEG oxidation. (c) Normalized radar chart of dual-mode (absorbance: A and fluorescence: FL) signals across different pH values.

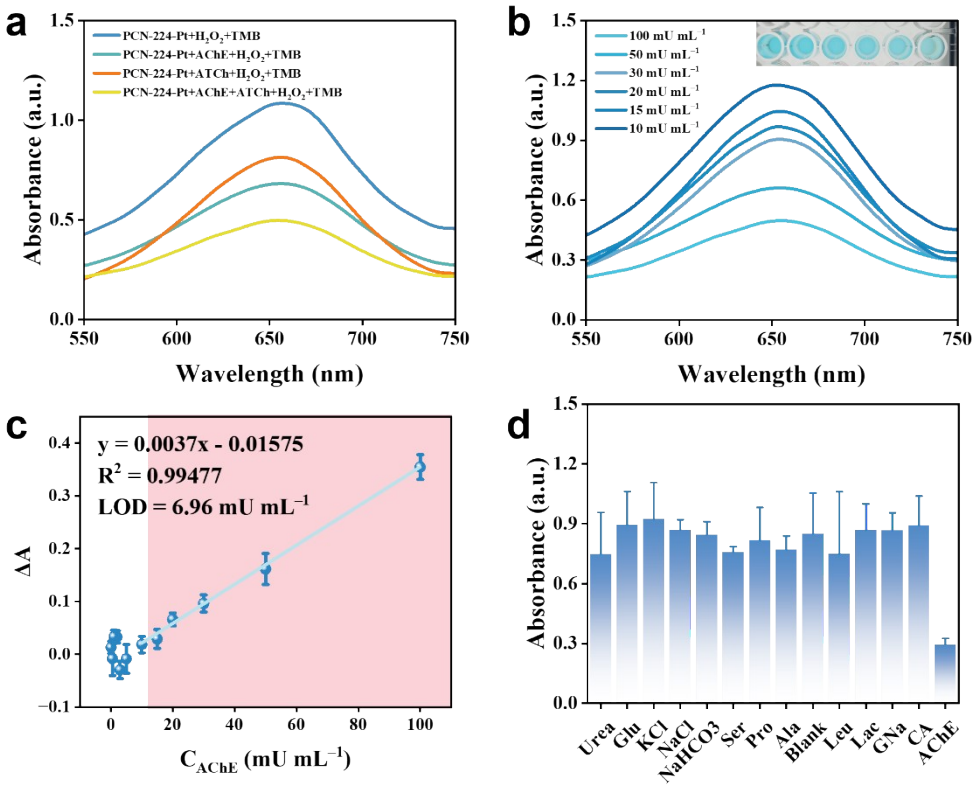

Figure S22. (a) Feasibility evaluation of the sensing platform using TMB as the chromogenic substrate. (b) Absorbance spectra at 652 nm for different AChE concentrations. (c) Calibration curve of absorbance change ($\Delta A = A - A_0$) versus AChE activity (0–100 mU mL^{-1}). (d) Selectivity evaluation against potential interfering species.

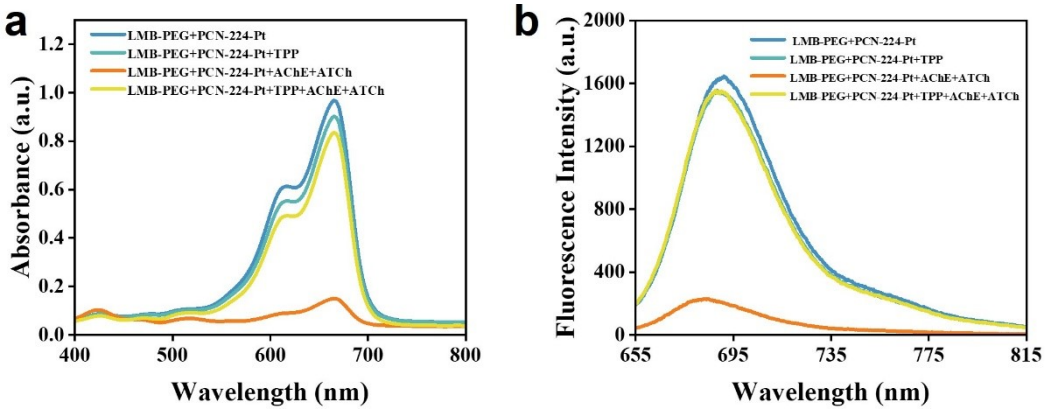

Figure S23. Feasibility of the PCN-224-Pt sensing platform to detect TPP using LMB-PEG as substrate, evaluated under (a) colorimetric mode and (b) fluorescence mode.

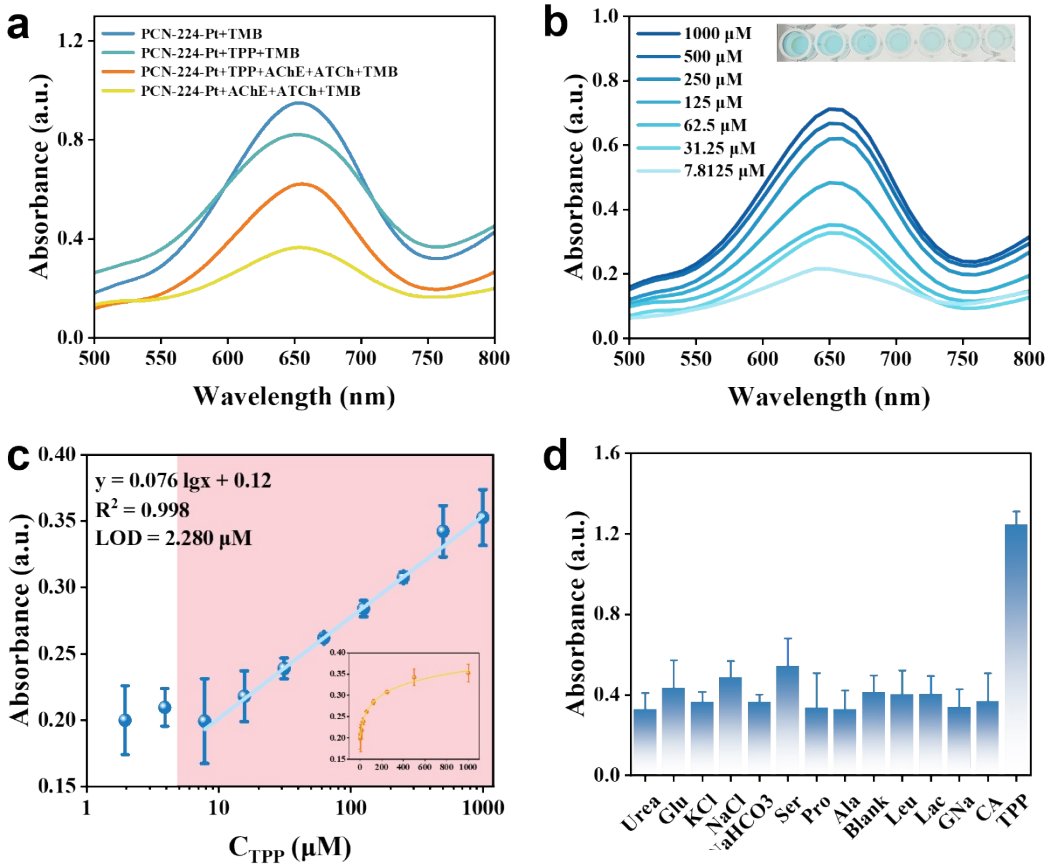

Figure S24. (a) Feasibility evaluation of the sensing platform using TMB as the chromogenic substrate. (b) UV–vis spectra at 652 nm for different TPP concentrations. (c) Calibration curve of ox-TMB absorbance versus TPP concentration (0–1000 μM). (d) Selectivity evaluation against potential interfering species.

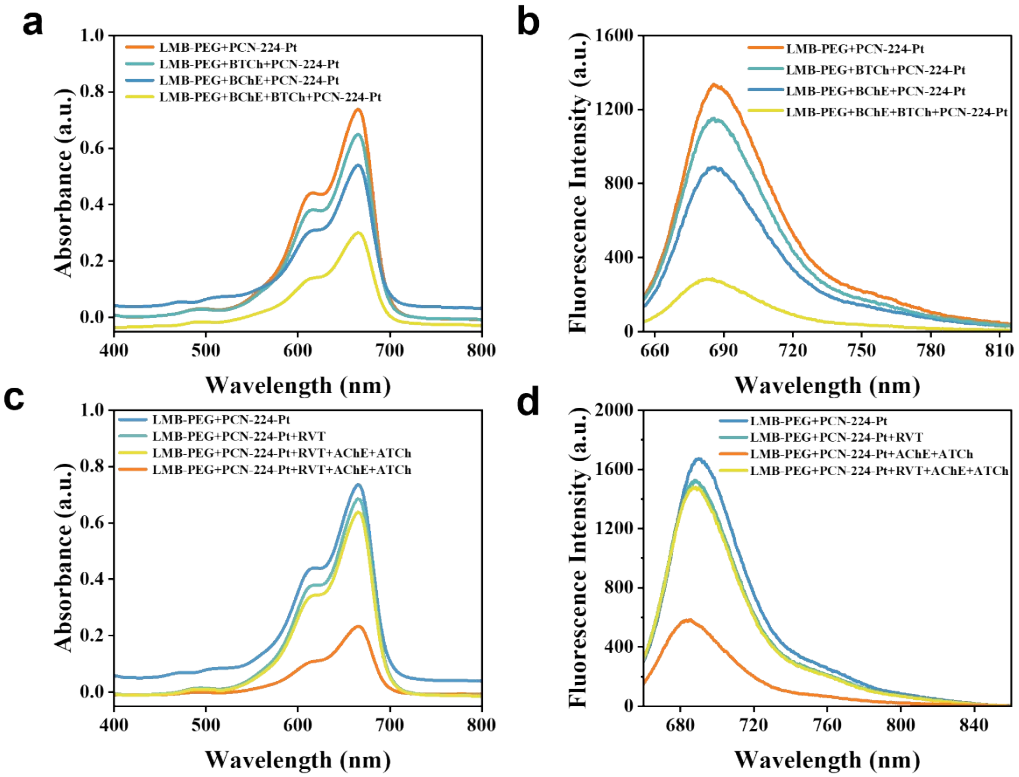

Figure S25. Feasibility of the PCN-224-Pt sensing platform for BChE and RVT detection using LMB-PEG as the substrate: (a, b) colorimetric and fluorescence detection of BChE, respectively; (c, d) colorimetric and fluorescence detection of RVT, respectively.

Table S1. Comparison of the Michaelis-Menten constant (K_m) and maximum reaction rate (V_{max}) of PCN-224-Pt with HRP and other POD-like nanozymes.

Nanozymes	K_m (10^{-3} M)		V_{max} (10^{-8} M s^{-1})		Ref.
	TMB	H_2O_2	TMB	H_2O_2	
PCN-224-Pt	0.14	0.16	28.11	76.93	This work
HRP	0.434	3.70	10.00	8.71	2
PCN-224-Fe	0.404	23.52	36.23	43.09	3
MIL-53(Fe)	1.08	0.04	8.8	1.9	4
Co-MOFs	0.41	0.97	17.6	14.3	5
Co/Fe-MOFs	3.51	5.37	7.63	2.71	6
ZIF-8/Au	0.1	0.27	3.85	3.88	7
Pt NPs@ZIF	0.15	66.78	0.12	0.26	8

Table S2. Comparison of the specific activity (SA) of PCN-224-Pt with other Pt nanozymes.

Nanozymes	SA (U mg^{-1})	Ref.
PCN-224-Pt	90.838	This work
PtNi NWs	10.43	9
Pt_c	12.4	10
m-Pt	46.2	11
$Pt_{50}Sn_{50}$	2.28	12
Ti_3C_2Tx-Pt-PEG	1.78	13
$CuCo_2S_4$-Pt-PEG	1.55	14
L10 PtCo@Pt	25.545	15
Pt_9Co	9.10	16

Table S3. Comparison of various detection methods for acetylcholinesterase (AChE) activity.

Method	Materials	Linear range (mU mL^{-1})	LOD (mU mL^{-1})	Ref.
Colorimetry/ Fluorometry	PCN-224-Pt	1–100 0.1–15	0.037 0.4469	This work
Colorimetry	CoN_x-NC	2.5–25	0.9	17
Colorimetry/ Photothermal	Fe-N-C	3–40	1.9 2.2	18
Colorimetry	PdSP@rGO	0.25–5	00.0625	1
SERS	AuNPs/NE	20–4800	20	19
Fluorometry	SiNPs@CuNCs	0–50	3	20
Colorimetry/ Fluorometry	BSA-CeO_2	0.1–25	0.081 0.056	21
Colorimetry	Au@CoAl-LDH-m	1–100	0.092	22
Colorimetry	2D Zn-TCPP(Fe) NSs	0.53–3.93	0.029	23
Colorimetry	BP QDs	0.5–10	0.17	24

Table S4. Spike recovery of AChE in human serum.

Method	Sample	Added (mU mL^{-1})	Measured (mU mL^{-1})	Recovery (%)	RSD (%, n=3)
Colorimetry	Sample 1	4.0	4.18	104.5	2.8
		50.0	51.05	102.1	1.5
		75.0	73.52	98.0	1.2
	Sample 2	4.0	4.26	106.5	3.1
		50.0	50.68	101.4	1.6
		75.0	76.89	102.5	1.4
Fluorometry	Sample 1	0.5	0.56	112.0	5.2
		7.5	7.95	106.0	2.5
		12.0	12.74	106.2	2.2
	Sample 2	0.5	0.48	96.0	4.8
		7.5	7.34	97.9	2.7
		12.0	11.43	95.2	2.4

References

1. L. Gao, J. Zhuang, L. Nie, J. Zhang, Y. Zhang, N. Gu, T. Wang, J. Feng, D. Yang, S. Perrett and X. Yan, *Nat. Nanotechnol.*, 2007, **2**, 577–583.
2. X. Lai, R. Li, B. Zhang, T. Zhang, X. Ji, L. Wang, Y. Cui, H. Xiao and D. Ning, *Colloids Surf. A*, 2024, **680**, 132645.
3. L. Ai, L. Li, C. Zhang, J. Fu and J. Jiang, *Chem. Eur. J.*, 2013, **19**, 15105–15108.
4. H. Wan, Y. Wang, J. Chen, H. M. Meng and Z. Li, *Microchim. Acta*, 2021, **188**, 130.
5. X. Zhao, J. Liu, F. Xie, T. Yang, R. Hu and Y. Yang, *Spectrochim. Acta A*, 2021, **262**, 120117.
6. Z. Zhu, X. Wang, N. Wang, C. Zeng, L. Zhang, J. Fan, X. Yang, P. Li, H. Yuan, Y. Feng, S. Huo and X. Lu, *Anal. Bioanal. Chem.*, 2024, **416**, 4417–4426.
7. M. Xia, S. Chu, S. Wang, X. Dong, C. Chen, Y. Jiang, Z. Li and Y. Lu, *Anal. Bioanal. Chem.*, 2023, **415**, 649–658.
8. J. Guo, C. Dong, X. Zhang, Y. Liu, Y. Leng, G. Wang and Z. Chen, *Anal. Chim. Acta*, 2024, **1321**, 343039.
9. Y. Chen, L. Jiao, H. Yan, W. Xu, Y. Wu, L. Zheng, W. Gu and C. Zhu, *Anal. Chem.*, 2021, **93**, 12353–12359.
10. Y. Zhang, Y. Kang, X. Wei, C. Chen, Y. Zhai, C. Zhu, L. Jiao, X. Lu and Y. Yamauchi, *ACS Nano*, 2025, **19**, 24013–24022.
11. Y. Zhu, R. Zhao, L. Feng, C. Wang, S. Dong, M. V. Zyuzin, A. Timin, N. Hu, B. Liu and P. Yang, *ACS Nano*, 2023, **17**, 6833–6848.
12. Y. Zhu, Z. Wang, R. Zhao, Y. Zhou, L. Feng, S. Gai and P. Yang, *ACS Nano*, 2022, **16**, 3105–3118.
13. M. Xu, R. Zhao, B. Liu, F. Geng, X. Wu, F. Zhang, R. Shen, H. Lin, L. Feng and P. Yang, *Chem. Eng. J.*, 2024, **491**, 151776.
14. B. Xu, M. Cui, Z. Luo and L. Wang, *Chin. Chem. Lett.*, 2025, 111227.

15. H. Shen, S. Chen, S. Mo, H. Huang, H. Liang, J. Zhang, Z. Xu, W. Liu and Y. Liu, *Adv. Funct. Mater.*, 2025, **35**, 2418360.
16. Q. Wang, Q. Li, Y. Lu, X. Zhang and Y. Huang, *ACS Sustainable Chem. Eng.*, 2021, **9**, 7668–7677.
17. L. Lu, X. Hu, R. Zeng, Q. Lin, X. Huang, M. Li and D. Tang, *Anal. Chim. Acta*, 2022, **1229**, 340383.
18. B. Yan, W. Liu, G. Duan, P. Ni, Y. Jiang, C. Zhang, B. Wang, Y. Lu and C. Chen, *Microchim. Acta*, 2021, **188**, 162.
19. Y. Chen, W. Zhao, J. Si, Y. Zheng, H. Tan, F. Meng, G. Yang, Y. Gu and L. Qu, *Anal. Chim. Acta*, 2022, **1232**, 340495.
20. X. Wen, F. Li, Y. Wang and Z. Fan, *Microchem. J.*, 2023, **194**, 109367.
21. Y. Dai, W. Xu, X. Wen, H. Fan, Q. Zhang, J. Zhang, H. Zhang, W. Zhu and J. Hong, *Microchim. Acta*, 2024, **191**, 185.
22. X. Yu, L. Zhang, X. He, W. Bai, H. Tan, Q. Li, Y. Shen, Y. Luo, Y. Yao, S. Li, H. Bai, J. Hu, W. Zhuang, L. Chen, X. Sun and W. Hu, *Inorg. Chem.*, 2024, **63**, 24065–24070.
23. Y. Wang, Y. Xue, Q. Zhao, S. Wang, J. Sun and X. Yang, *Anal. Chem.*, 2022, **94**, 16345–16352.
24. L. Ren, H. Li, M. Liu and J. Du, *Analyst*, 2020, **145**, 8022–8029.